

Controls on grain size distribution in an ancient sand sea

Gabriel Bertolini

gabertol@gmail.com

Universidade Federal do Rio Grande do Sul, Brazil

@Gabertol_

Adrian John Hartley

University of Aberdeen, U.K.

@adrian_hartley

Juliana Charão Marques

Universidade Federal do Rio Grande do Sul, Brazil

Jhenifer Caroline da Silva Paim

Universidade Federal do Rio Grande do Sul, Brazil

Abstract

Grain size distribution in deserts is driven by a combination of autogenic controls such as grain abrasion and sorting due to wind transport and allogenic controls such as provenance and spatial changes in wind-direction. Downwind grain-size trends in present day sand seas display contrasting results. For example, the Namib and Hexi Corridor sand seas show broad downwind fining and sorting trends which are not present in the Ténéré, Australian and Sinai sand seas. This study examines the grain size distribution along the margins of the Cretaceous Botucatu paleodesert across an area of >1,000,000 km² to determine the relative importance of autogenic and allogenic controls on sand distribution. A comparison between the spatial distribution of grain size metrics with detrital zircon geochronology as a provenance test, paleowind patterns as a wind-regime test and 3 transects along the basin paleomargins as a downwind abrasion test, are used to quantify the main controls on Botucatu paleodesert grain-size distribution. Grain size dispersion shows an E to W fining pattern, which agrees with provenance control - in contrast to a N-S trend expected for the predominant wind-regime control. In the NE region there is good evidence for downwind fining due to aeolian abrasion – of about 0.4 μm by km, indicating that whilst downwind fining due to abrasion does occur, but that it is limited by the rounded nature of available sands for Botucatu desert and possibly by mix of different provenance sources. The results suggests that the provenance of the available sand is the primary control on the grain-size distribution in the Botucatu sand sea and potentially in most large-scale dune fields.

1. Introduction

The construction of dune fields by aeolian system is ruled by a set of external (allogenic) and internal (autogenic) forces. Autogenic forces account for the granular self-organization tendency within natural sedimentary systems (Kocurek and Ewing, 2005; Werner, 1999, 1995). Allogenic controls correspond to external environmental drivers that are linked to external forces such as tectonism, climate or base-level changes (Jerolmack and Paola, 2010; Rodríguez-López et al., 2014). Jerolmack et al. (2011) propose that grain-size distributions in aeolian environments are derived from coupled sorting and abrasion due to the saltation of grains in the downwind direction. Abrasion during transport is inherent to the aeolian system (Bagnold, 2016; Bullard et al., 2004a; Durian et al., 2006; Kuenen, 1960), suggesting an autogenic control on grain size distribution. However, studies on grain size distribution in modern sand seas find conflicting patterns (Bristow and Livingstone, 2019; Lancaster, 1986, 1985, 1981; Langford et al., 2016; Liang et al., 2020; Livingstone et al., 1999; Wang et al., 2003; Zhou et al., 2021). For instance, in SW Namibia (Lancaster, 1989), the White Sands in New Mexico (Jerolmack et al., 2011), and the Hexi Corridor in China (Zhang and Dong, 2015) fining and sorting downwind patterns occur over scales of 10's of kms. In contrast, in the Kalahari in Namibia (Lancaster, 1986), the Ténéré in the Sahara (Warren, 1972), the Gibson Desert in Australia (Buckley, 1989) and the Sinai (Sneh and Weissbrod, 1983) no downwind grain-size patterns were identified in dunefields. Langford et al. (2016) found evidence that mixing of sand sources in White Sands provided additional controls on dune-field grain-size distribution in contrast to the simple downwind fining and sorting processes proposed by Jerolmack (2011) for the same desert. Among these additional controls, wind-regime and the provenance of the available sands are related to external controls on the grain size dispersion. In summary, the spatial distribution of grain size within desert sands is a combination of the inherent organization patterns in natural granular systems and the available external conditions.

In the sedimentary literature, there is lack of studies that quantify the role of allogenic and autogenic factors that control grain size distribution in aeolian strata at a basinal scale ($>500.000 \text{ km}^2$). Our work aims to address this issue using the Botucatu paleoerg as a case study. The Botucatu paleoerg is a large-scale ($>1.000.000 \text{ km}^2$) dune-field developed in W Gondwana during the Early Cretaceous. Two main allogenic factors

are hypothesised to influence the development of the Botucatu paleoerg: (1) a wind-direction zoning due to the monsoonal climate in Gondwana (Bigarella and Oliveira, 1966; Bigarella and Salamuni, 1961; Scherer and Goldberg, 2007a); (2) a provenance variation derived from the recycling of underlying strata from the Paraná Basin (Bertolini et al., 2021, 2020). Changes in grain size and sorting in a downwind direction can be related to aeolian abrasion, which is intrinsic to the aeolian system and should therefore represent an autogenic signal. To determine the relative roles of auto- and allogenic controls on grain size dispersion in deserts, we apply 3 independent tests using multiproxy datasets: (1) provenance spatial changes using detrital zircon, (2) spatial distribution of wind directions utilising paleocurrent data and (3) changes in grain-size across a number of transects. The tests are used to check and compare (a) the directionality and (b) the magnitude of each mechanism in influencing grain-size dispersion. Ultimately, the paper aims to develop a model that utilises the grain size distribution to test the importance of allogenic factors, represented by the wind-direction and provenance zoning, and autogenic factors, evaluated using downwind changes along transects.

2. Background

2.1 Deserts grain-size distribution

The grain size distribution in deserts sands has been the focus of studies since the seminal work of Bagnold documented in the “Physics of the blowing sand”. Since the late 1970s, the spatial distribution of grain-size within modern deserts has been studied extensively by Lancaster (Lancaster, 1982, 1981) who pioneered descriptive granulometry analysis in the SW Africa Kalahari and Namib dune fields. Later, several deserts were the focus of grain size studies, such as ergs in China – Taklimakan, Hexi Corridor, Kumtagh (Liang et al., 2020; Wang et al., 2003; Zhang and Dong, 2015), Africa- Namibia, Kalahari, Sinai, Tenéré- (Bullard et al., 1997; Lancaster, 1985, 1981; Livingstone, 1987; Livingstone et al., 1999; Thomas, 1988; Watson, 1986), and Australia- Strzelecki, Simpson- (Buckley, 1989; Thomas, 1988). These studies focussed on a the grain-size distribution under distinct scale perspectives: (1) differences of grain-size within single dunes; (2) comparison of grain-size between individual regions of different dunes such as crests, flanks, plinth or interdune; and (3) grain size changes at km scales across large-scale deserts ins downwind direction.

Overall, there are contrasting findings on grain size distribution at all scales (Bristow and Livingstone, 2019; Langford et al., 2016). At the dune and dune comparison scale, studies in the Namib, Kalahari, Taklimakan and Australian ergs show that dune crests

can be finer (Livingstone, 1987; Watson, 1986), coarser (Thomas, 1988; Wasson, 1983) or equal in grain size to interdunes (Livingstone et al., 1999; Sneh and Weissbrod, 1983; Wang et al., 2003). At the desert scale (>30,000 km²) (Wilson, 1973), some studies suggest modifications in grain size attributes along the sand transport direction. Lancaster (1989) found a decrease in grain size and skewness and an increase in sorting along a south to north trend in the Namib Sand Sea - which corresponds to the overall transport direction (Garzanti et al., 2012). Studies in the Hexi corridor desert also found upwind to downwind fining of mean grain size (Zhang and Dong, 2015). Studies in the Kalahari desert produced conflicting results, Lancaster (1986) describes finer and better-sorted sands along a NE-SW transport trend, whereas Livingstone et al. (1999) found no trend in granulometry statistics along a 28 km transect. A similar issue occurs in the White Sands dune field in New Mexico, where (Langford et al., 2016) found evidence of source mixtures influencing grain size trends using end-member mixtures, whereas Jerolmack et al. (2011) proposed a downwind autogenic abrasion control on the fining and sorting in the dunefield. The large-scale ergs of Ténéré, Gibson and Sinai (>30,000 km²) also display negligible to no spatial variations in grain size distribution (Buckley, 1989; Sneh and Weissbrod, 1983; Warren, 1972). In some cases, the fluvial-aeolian interactions can provoke a mixture of sources. For instance, the Kumtagh Sand Sea in NW China, displays a relationship between grain-size distribution and fluvial-aeolian processes, in which downwind fining occurs, but also a mixture of upwind and locally-derived sands, produces a mixture of zones controlled by either aeolian or fluvial sands (Liang et al., 2020).

In summary, studies from modern sand seas provide a range of different results in assessing the controls on grain-size distribution within dune- and erg-scale desert systems. Thus, the nature of grain-size distribution and its relationship with aeolian transport and sand source is still not well established.

2.2 Botucatu paleoerg

The Botucatu paleoerg covered an area of up to 1500000 km² in Western Gondwana (Figure 1 inset), and is preserved in South America and SW Africa. The paleodesert is represented by a vast and thick (up to 400 m) sandstone unit referred to as the Botucatu Formation (Brazil), the Rivera Member (Uruguay), and the Twyfelfontein Formation (Namibia). The unit typically outcrops as stacked large cross-stratified sandstones, interpreted to be formed by the superimposition of crescentic and linear dunes in a dry-aeolian system (Scherer, 2002, 2000; Scherer and Goldberg, 2007a). Its

age is constrained at the top by radiometric dates from the synchronous continental flood basalts of the Paraná-Etendeka large igneous province that have ca. 134 Ma age (Baksi, 2018; de Assis Janasi et al., 2011; Ernesto et al., 1999; Pinto et al., 2011; Thiede and Vasconcelos, 2010). Desert onset is believed to be Early Cretaceous due to the ichnofossil assemblage (Francischini et al., 2015).

Provenance studies show that recycled sands were prevalent along the desert margins, mainly sourced from underlying Paraná Basin strata. In detail, (Bertolini et al., 2020) suggest that a change in provenance occurred from SW to SE in the desert based on provenance proxies - particularly the Cambrian-Neoproterozoic detrital zircon contribution. Detrital zircon signatures from the northern area of the Botucatu suggest a northwestern to northeastern provenance change (Bertolini et al., 2021). Overall, the Botucatu sands result from intense intrabasinal reworking of underlying Paraná Basin strata (Bertolini et al., 2021, 2020); with evidence for East to West shifts in provenance governed by the spatial distribution of underlying Paraná Basin strata.

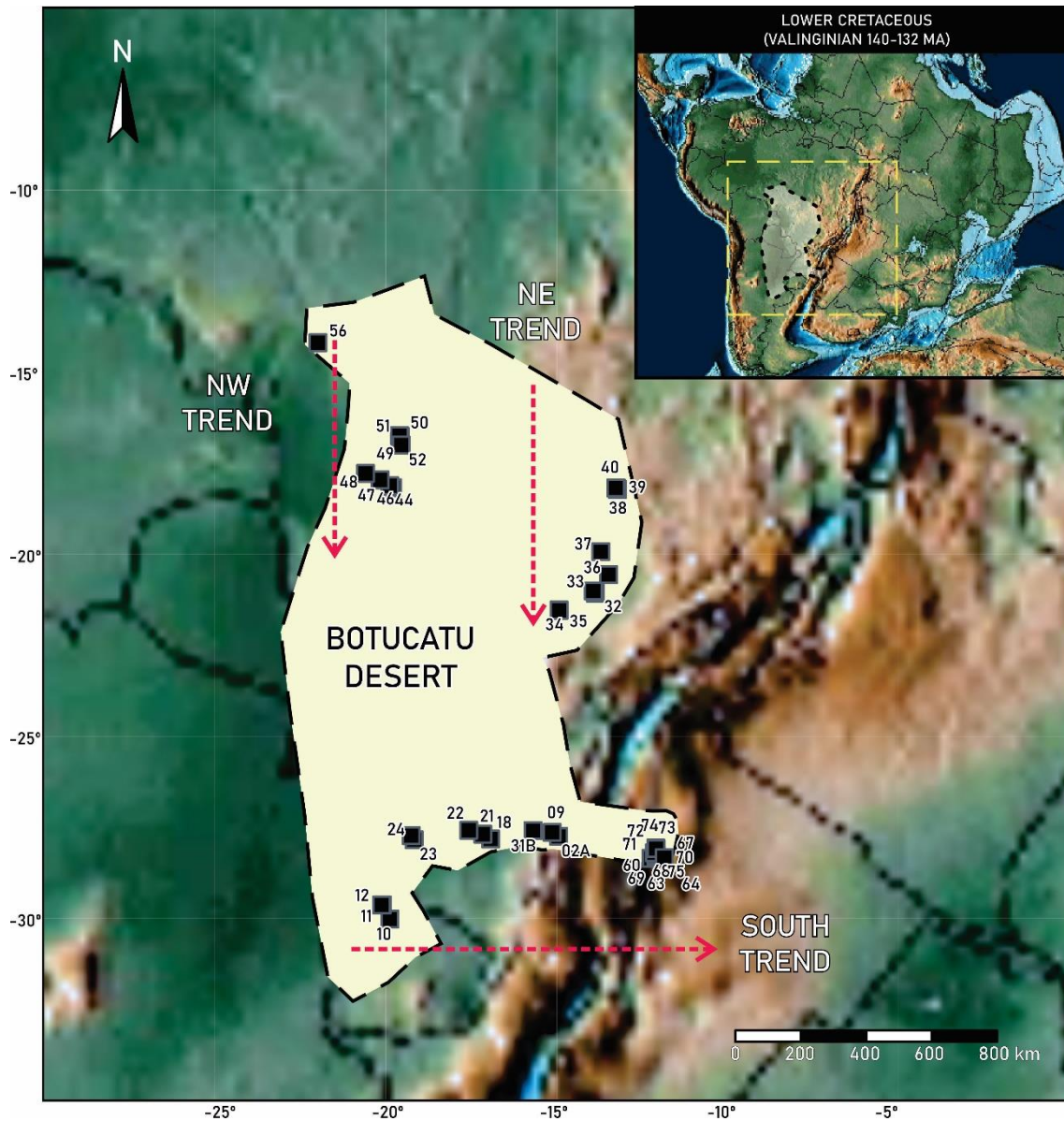


Figure 1 – Grain-size sampling sites (table 1) and transects (Northwestern, northeastern and south).

3. Methodology

This study utilises forty-one sand samples in thirty-nine sites in Brazil, Uruguay and Namibia (Figure 1). The samples were collected in outcrops from cross-stratified sandstones deposited as aeolian dunes. Cross-stratified facies were selected to avoid or limit dune position grain size bias. We present 12 new samples collected in outcrops in Namibia, in addition to previously published data in South America (Bertolini et al., 2021,

2020). Table 1 compiles the samples by location, grain-size metrics, wind direction (based on the model from figure 3), and literature sources.

Granulometry data were acquired using classical sieving methods for the sand grain-size (0.0625 to 2.00 mm) in Centro de Pesquisa Costeira from Universidade Federal do Rio Grande do Sul. Around 100 g of samples were softly disaggregated, to avoid grain breakage, with rubber pestle and dried in an oven (<100°C). The dry samples then were wet sieved using 5 grain classes (0, 1, 2, 3, 4 phi). The samples were dried again and individually weighed. Silt and clay granulometry consists of a mixture of detrital grains and fine cement, so we selected only the sand fraction. Mean grain-size, sorting, skewness and kurtosis have been calculated using geometric method of moments by (Folk and Ward, 1957), using the R package G2Sd (Fournier et al., 2014)- which is an R implementation of the Gradistat spreadsheet (Blott and Pye, 2001) for granulometry calculation.

The analysis was run in R (R Core Team, 2021) in RStudio Software (<https://www.R-project.org/>). Data manipulation, wrangling and plots were made using the tidyverse package (Wickham and Wickham, 2017), coordinate transformation to the Early Cretaceous reference frame was undertaken using the chronosphereR package (Kocsis and Raja, 2020), spatial data handling and analysis with SF and SP packages (Pebesma and Bivand, 2005; Pebesma, 2018), interpolation with automap (Hiemstra, 20XX). The Full code applied here is available at Github <https://github.com/gabertol?tab=repositories>.

4. Results

The grain-size distribution for dunes from the Botucatu Desert are displayed in figure 2. Mean grain size, sorting, kurtosis and skewness were calculated using the geometric method (Folk and Ward, 1957) in millimetres, following the suggestion of (Blott and Pye, 2001). The dataset displays a mean grain-size ranging from 1.05 to 0.05 mm (mean 0.3 mm), sorting from 2.12 to 1.45 (mean 1.68 μ m), skewness from 0.57 to -0.35 (mean -0.11 μ m) and kurtosis from 1.56 to 0.74 (mean 0.99 μ m). Overall, the sands are medium grained, moderately sorted, mesokurtic and symmetrical to fine skewed.

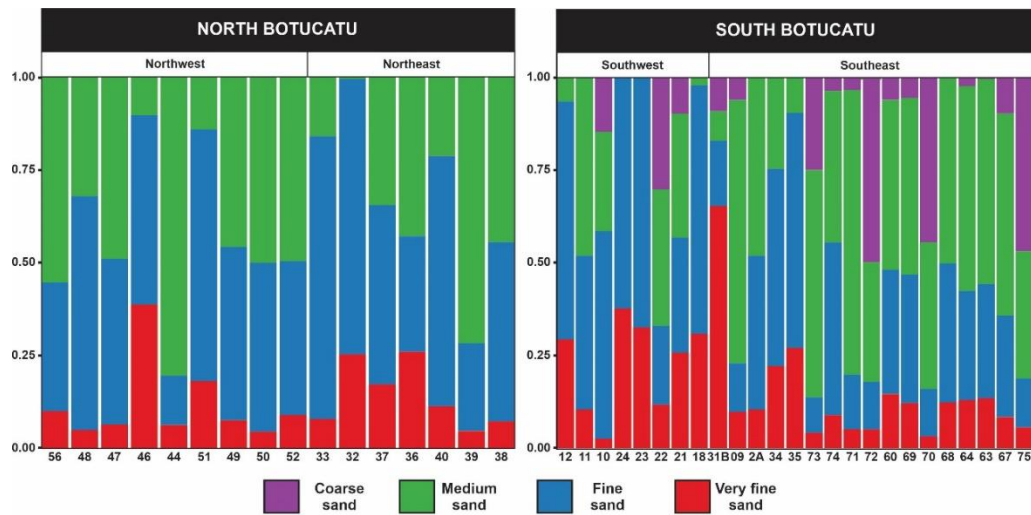


Figure 2 - Grain-size distribution and wind-direction for Botucatu desert samples.
 Samples ordered from west to east

In detail, the granulometry display differences based on spatial patterns. Figure 3 displays probability functions from sands from the north and south of the desert, based on the wind model (section 4.1 and figure 3). The mean grain size, sorting and skewness (Fig.4 A,B,C) shows different averages from south to north. The north Botucatu area records fine-sands (mean 0.23 mm), moderately well sorted (mean 1.60 mm), and symmetrically skewed (mean -0.09 mm). The south Botucatu sands are medium (mean 0.35 mm), moderately sorted (mean 1.73 μ m) and fine-skewed (mean -0.12 μ m). Overall, the southern Botucatu material has coarser and more poorly sorted sands, and consequently, is positively skewed.

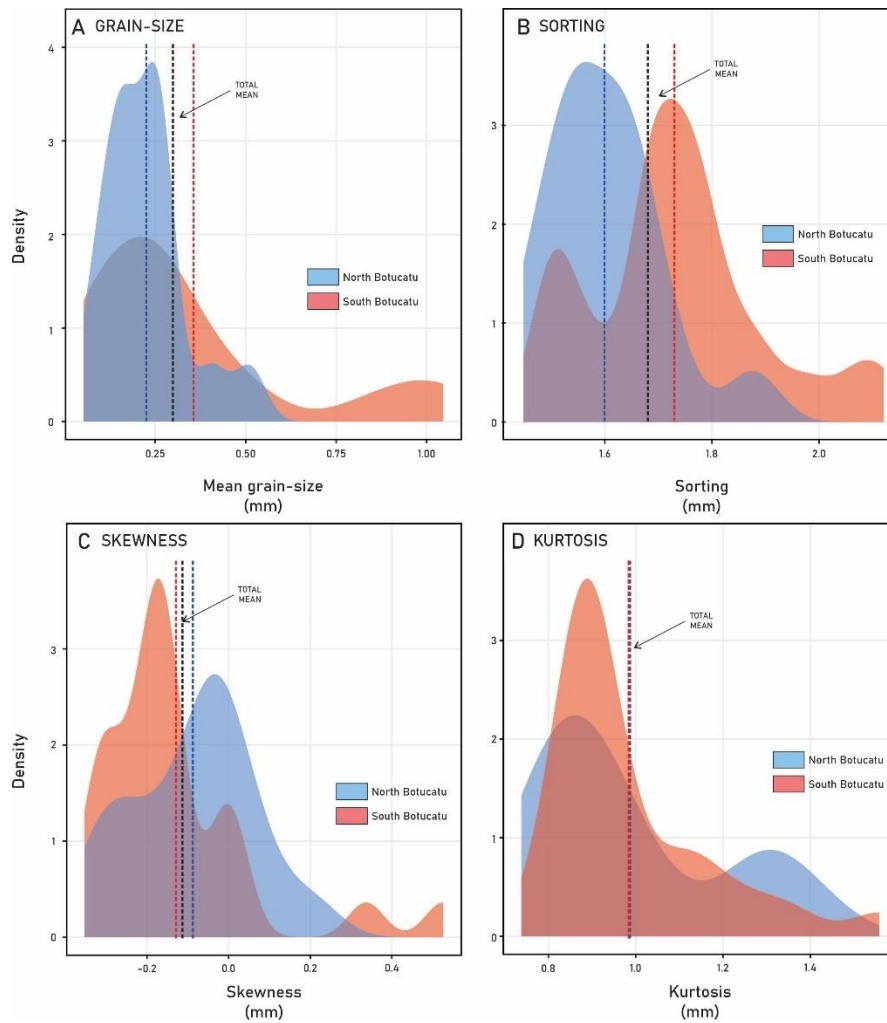


Figure 3 - Grain-size metrics probability density functions illustrating the dunes from the north and south of Botucatu paleodesert. Red- and blue dashed lines represents south and north Botucatu, respectively. (a) mean grain-size, (b) sorting, (c) skewness, and (d) kurtosis.

Figure 3 shows the changes in granulometry based on region such that spatial changes may be assessed through interpolation. The grain-size metrics have been interpolated with the ordinary kriging method (figure 4). The mean grain size (Fig. 4A) shows a dominant trend of coarser sand from SW-NE, from 0.38 to 0.10 mm. The S.W. region which is located in southeast Brazil and Namibia, comprises the coarsest sands in the desert. Kurtosis, skewness and sorting (Fig.4 B, C, D) show minor trends- from 50 to 100 km, where high kurtosis, low skewness and low sorting overlap. Overall, the sands are medium in size, moderately sorted, mesokurtic and symmetrical to fine skewed.

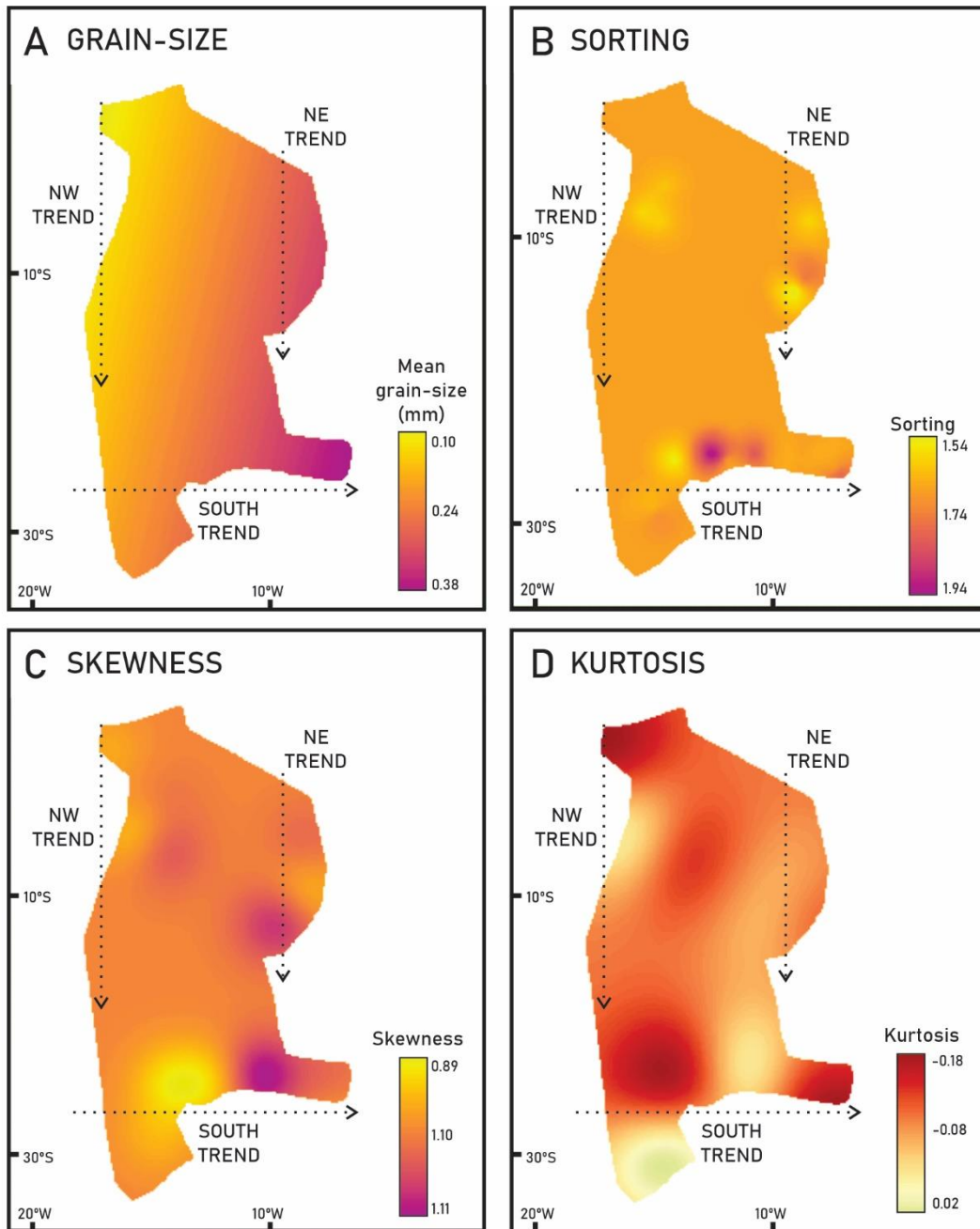


Figure 4 – (A) Mean grain-size (mm); (B) Sorting; (C) Skewness; (D) Kurtosis ordinary kriging models.

The analysis reveals trends in granulometry metrics, in particular the mean grain-size. To test the influence of the hypothetical allogenic and autogenic mechanisms on grain size spatial distribution, three independent tests have been set up. The wind-direction test (4.1), provenance test (4.2), downwind trend test (4.3) are used to evaluate respectively the allogenic (wind-regime and the sand-sources) and autogenic (downwind abrasion) forces. The wind-direction (4.1) model is used to model the wind spatial distribution and classify the predominant wind direction for each granulometry sample. The provenance test (4.2) aims to model the spatial distribution of sand sources using 21 samples of detrital zircon. The downwind trend test (4.3) presents

linear models for downwind mean grain-size changes across three trends (northeastern, northwestern and south transects) to check the abrasion along wind transport.

4.1 Wind-direction test

Studies of the Botucatu desert show that it records a complex wind pattern (Bigarella and Oliveira, 1966; Bigarella and Salamuni, 1961; Bigarella and Van Eeden, 1970; Scherer, 2000; Scherer and Goldberg, 2007a). Three main zones of prevalent wind-direction are documented: a North, South and a mixed zone. The North Botucatu zone is located from 12°S to 20°S (present day latitudes) with a mean wind direction of $232 \pm 12^\circ$. The South Botucatu wind-zone occurs between 33°S to 25° S (present day latitudes), and a mean direction of $71 \pm 6^\circ$. The mixed zone is located in the central Botucatu (12°S to 20°S) with polymodal winds directions, presenting a mixture of wind-directions typical for North and South desert. To evaluate the prevailing wind direction across the desert in order to compare with the grain size data, we interpolate paleocurrents from published work (Bigarella and Oliveira, 1966; Bigarella and Salamuni, 1961; Bigarella and Van Eeden, 1970; Mountney and Howell, 2000; Scherer, 2000; Scherer and Lavina, 2006; Silva and Scherer, 2000). Wind direction vector directions from forty-nine sites were compiled and modelled using the inverse distance weighted algorithm. Figure 2 displays the inverse distance weighted model for the Lower Cretaceous Gondwana wind direction and histogram with the distribution of the direction. Table 2 compiles the site locations, mean direction, the confidence interval, and sources. The mean vector directions and confidence intervals follow the equations of (Scherer and Goldberg, 2007a).

The North Botucatu area registers mean winds blowing to the S-SW, and the South Botucatu shows prevailing winds blowing towards the eNE. In terms of mode, the wind directions are 73° and 174° . The zone from 20°S to 25°S shows a mixture from both dominant winds, but mostly from northern winds. The model agrees with previous paleowind studies for the Botucatu Desert (Scherer and Goldberg, 2007a) and global circulation models (Moore et al., 1992) that display a monsoon bimodal wind pattern over West Gondwana.

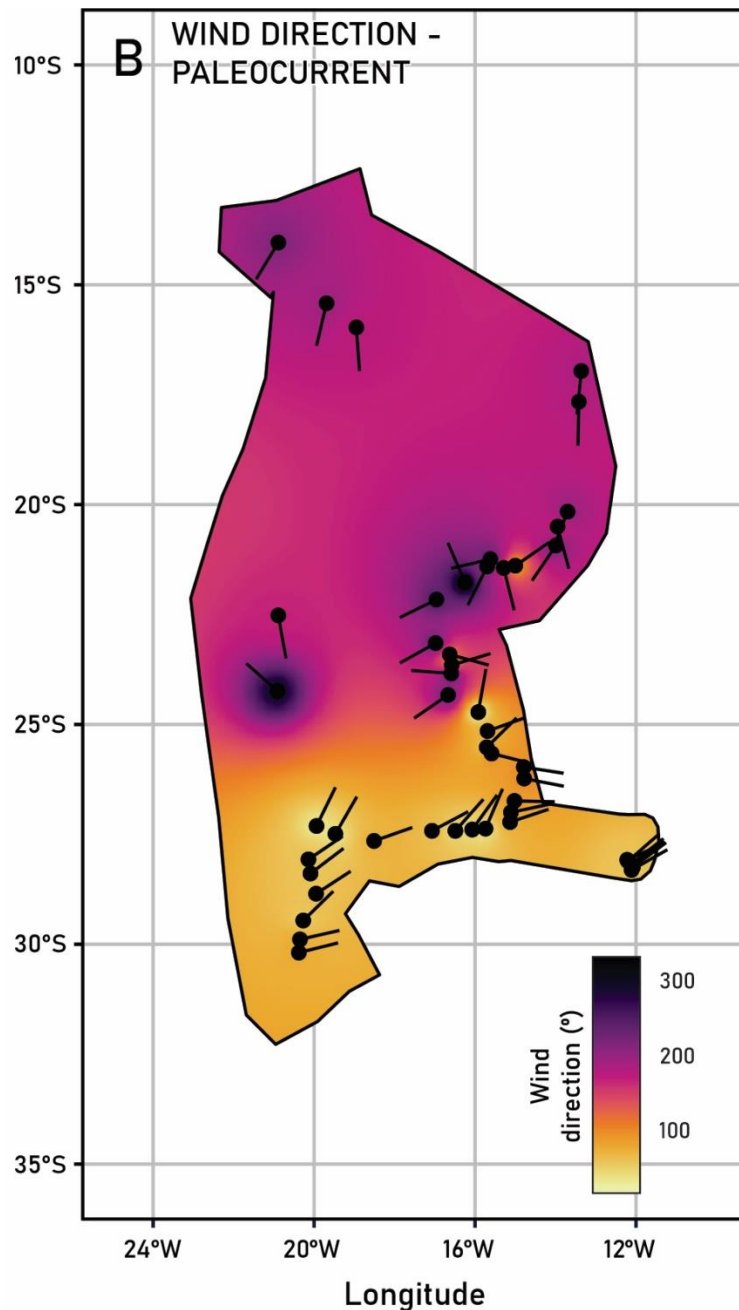


Figure 5- Inverse distance weight model for Botucatu desert wind-directions. The wind direction distributions shows a dominant $71\pm 6^\circ$ wind in south Botucatu, and $232\pm 12^\circ$ in north Botucatu.

4.2 Provenance test

The Botucatu paleoerg has been the focus of several detrital zircon U-Pb dating studies (Bertolini et al., 2021, 2020; Canile et al., 2016, Peri et al., 2016, Zieger et al., 2020). We compile 3,975 U-Pb detrital ages from 44 samples from Brazil, Uruguay, Argentina and Namibia. The detrital zircon studies have polymodal distributions, so an appropriate form of representation of their relationships are made using dimensional reduction techniques. An approach widely applied in sedimentary provenance studies,

is to use multidimensional scaling plots (Vermeesch, 2013; Vermeesch and Garzanti, 2015). Dimensions 1 and 2 are the most significant, such that a ratio of them simplifies the results into a single proxy. Figure 5 displays the ordinary kriged interpolation with the provenance proxy, indicating a W to E trend in the desert provenance. This agrees with previous provenance studies, that found W-E trends in the provenance of the southern Botucatu Desert- mostly related to changes in the composition of the material in the underlying Paraná Basin strata.

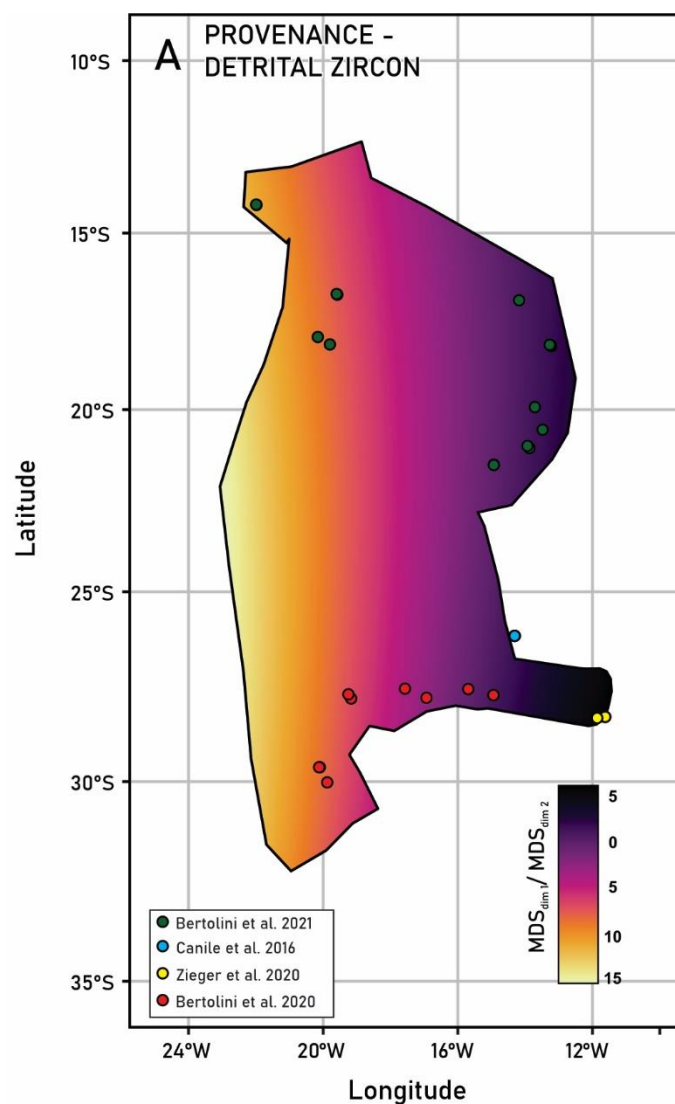


Figure 6- Ordinary kriged interpolation of provenance, using detrital zircon dataset from Bertolini et al., 2020, Bertolini et al. 2021, Zieger et al., 2020, Canile et al., 2016. The plotted values are a ratio of dimensions 1 and 2 of multidimensional scaling plot.

4.3 Downwind trend test

To evaluate the role of wind direction in controlling grain size distribution, we plot the mean grain size along three transects: northwestern, northeastern and south (Fig. 7). The transect locations are shown in figure 1. The trends vary over hundreds of kilometres. The longitudinal trends correspond to west to east distances, which are equivalent to upwind to downwind due the prevalent northeastern wind in the southern region. The latitude trends in the north region (northeastern and northwestern trends) correspond to N to S distances- equivalent to upwind to downwind in the northern Botucatu zone.

The Northeastern transect (Fig. 7A) displays a trend of grain-size fining related to paleolatitude changes in a downwind direction. In the northwestern region (Fig. 7B), there is no apparent relationship between latitude and grain size. Lastly, the south region (Fig. 7C) shows coarser sand toward the west, indicating an upwind fining trend. Linear models and statistics for each model are plotted in figure 5.

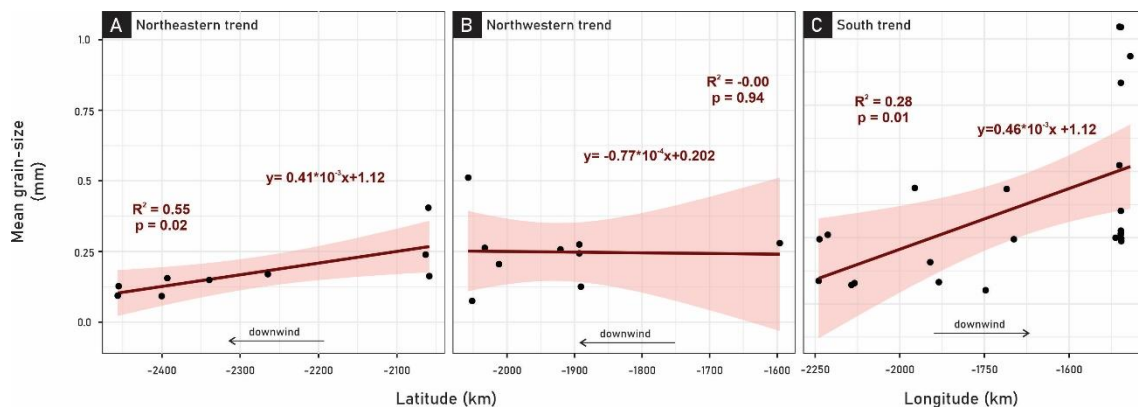


Figure 7 – A-C - Models for mean granulometry along regional transects across paleolatitude and paleolongitude distances. Pale-pink area represents standard error.

5. Discussion

The overall grain size distribution of the Early Cretaceous Botucatu desert comprises fine to medium, moderately sorted, symmetric to fine skewed and mesokurtic sands (figure 2 and 3). Table 2 compiles the granulometry statistics for several modern deserts, including the dune types, the sampling position and if there are any spatial changes within transects. The mean grain size found for Botucatu is coarser than registered in modern deserts, such as the SW Kalahari (Lancaster, 1986), Namib (Lancaster, 1981), Libya (Ahlbrandt, 1979), Simpson (Folk, 1971), Thar (Goudie et al., 1973) and Sinai (Tsoar, 1978). Additionally, the Botucatu is more poorly sorted than other deserts. The mean grain-size compared to other deserts is relatively similar, as

table 2 shows that deserts grain-size tend to be centred around 2 phi – corresponding to medium to fine sands. The sorting usually has values around 0.5 – considered to be well- to moderately sorted.

Table 1 – Granulometry metrics for deserts (values in phi)

desert	source	dune type	sample position	Trends	Mean grain-size	error	Sorting	error	Skewness	error	Kurtosis	error	
Botucatu	Bertolini et al. 2021 & Bertolini et al. 2020 & This study	crescentic, linear	paleodunes (cross-stratified sandstones)	NW no trend	2.17	0.11	0.68	0.02	0.09	0.05	0.96	0.08	
		crescentic, linear		NE downwind trend in grain-size	2.36	0.10	0.69	0.04	0.08	0.05	1.04	0.06	
		crescentic, linear		S downwind coarsening	2.03	0.11	0.79	0.03	0.14	0.04	0.98	0.04	
SW Kalahari	Lancaster 1986	linear dune	crest	Downwind fining and sorting	2.16	0.20	0.49	0.12	0.14	0.09	0.52	0.03	
					NE flank	2.21	0.19	0.62	0.16	0.05	0.12	0.52	0.02
					SW flank	2.26	0.18	0.59	0.15	0.07	0.09	0.53	0.04
Namib	Lancaster 1981	linear dune	crest	Dune facies changes - finer and sorted crest than plinth	2.44	0.15	0.37	0.10	0.17	0.13	0.54	0.04	
					base slip face	2.49	0.13	0.34	0.10	0.03	0.12	0.52	0.05
					mid slip face	2.32	0.14	0.40	0.11	0.05	0.18	0.52	0.04
					upper west slope	2.41	0.09	0.50	0.09	0.11	0.12	0.50	0.02
					east plinth	2.08	0.16	0.63	0.09	0.20	0.24	0.49	0.08
					west plinth	2.07	0.17	0.75	0.12	0.35	0.18	0.46	0.05
Skeleton Coast	Lancaster 1982	transverse and barchan ridges, and barchanoids	crest	Changes in dune types, facies and regional fining and sorting	2.02	0.25	0.51	0.26	0.28	0.19	0.50	0.05	
Lybia	Ahlbrandt 1979	linear dune	crest		2.37		0.46						
Canning Basin	Ahlbrandt 1979	linear dune	crest		2.02		0.53						
Simpson Desert	Folk 1971	linear dune	crest		2.53		0.43						
	Wasson 1983				1.62		0.30						
					2.90		0.81						
Thar Desert	Goudie 1973	linear dune	crest		2.65		0.56						
Sinai	Tsoar 1978	linear dune	crest		1.87		0.44						
Yarlung Zangbo	Zhou et al. 2021	barchans, transverse dunes, crescentic ridges and compound crescentic dunes	dune		2.12	0.26	0.61	0.18	0.04	0.07	0.97	0.05	
Algodones	Sweet et al. 1988	linear dunes	crest		2.49		0.37						
		transverse dunes	crest		2.53		0.39						
		draas	crest		2.49		0.34						
Kumtagh Sand Sea	Liang et al., 2020	linear dunes and compound (mega) star dunes (Dong)	crest	Downwind fining/ no sorting	2.9-1.6		0.8-0.2						
El Vizcaíno Desert	Kasper-Zubillaga et al., 2007	transverse	crest		2.59	0.03	0.45	0.04	0.06	0.01	1.05	0.04	
		barchan	crest		2.59	0.03	0.43	0.02	-0.02	0.03	1.04	0.04	
		transverse and barchan	crest		2.59	0.02	0.44	0.02	0.02	0.02	1.05	0.03	
White Sands	Langford et al. 2016	crescentic ridges, barcanoid and barchan, parabolic	dunes, and interdunes	Downwind sorting and minor fining	2.59-0.44		0.45-1.2						
					1.06								

The allogenic forces - i.e. wind-direction and provenance - show conflicting results. The wind-direction model (Fig. 5) shows that in the North and South Botucatu zones, contrasting wind-directions, blowing toward 174° and 73°, respectively occur. The central region of the desert displays a mixture of both northerly and southerly directed winds, with southerlies predominating. The model shown in Figure 5 agrees with previously published data (Bertolini et al., 2020; Moore et al., 1992; Scherer and Goldberg, 2007a), suggesting that winds derived from the northern hemisphere extended as far south as 30° S, due to the mega monsoon climate that dominated over Gondwana. The provenance test (Fig. 6) shows an E-W trend, which is compatible with the grain-size interpolation map (Fig. 4). Such trends are in agreement with Bertolini et al (2020) who found significant changes in detrital zircon and grain-size patterns along a West to East trend in southern Brazil.

The autogenic mechanism of wind-abrasion is examined in figure 6, which models the mean grain size along the downwind transects in the Northeastern, Northwestern and Southern regions. The Northeastern transect distribution is explained by a simple linear model (Fig. 7A), which finds $p=0.02$ and R^2 of 0.55. The model indicates a fining of 0.0004 mm per kilometre in mean grain size. There is no relationship between grain size and downwind distance in the northwestern region, as the figure 5B model shows. Along the southern transect a coarsening trend in a downwind direction is observed. The model (Fig. 7) finds a linear relationship with $p=0.01$ and R^2 of 0.28, with a coarsening of 0.46 μm in mean grain size per kilometre.

The fining trend in the northeastern region is similar to that found in other deserts, such as the Namib, Kalahari and Hexi Corridor deserts (Lancaster, 1986, 1981; Zhang and Dong, 2015). Other deserts such as the Ténéré, Sinai or Australian erg show no spatial grain size relationship (Buckley, 1989; Sneh and Weissbrod, 1983; Warren, 1972). , and this is also seen in the NW Botucatu region. In addition downwind coarsening occurs in the southern region. Our results indicate the existence of large-scale downwind abrasion in the northeastern region, however this is not seen elsewhere in the basin. Previous studies (Bullard et al., 2004b; Durian et al., 2007, 2006; Kuenen, 1960) shows that downwind abrasion should be expected, so additional controls must be acting on the NW and South regions. Langford (2016) suggested the existence of a mixture of sand sources in the White Dunes desert, interrupting and negating a long-distance trend of sand fining due wind abrasion. From this perspective, the northwestern Botucatu may record a greater mixing of sand sources than the northeastern desert.

The ordinary kriging model for the basin (Fig. 4) shows a general grain-size fining from E to W, ranging from 0.38 to 0.10 mm. This trend is on contrast to the regional northerly and southerly trending winds illustrating that the wind direction has limited effect on grain size distribution. Skewness, sorting and kurtosis interpolation shows local changes within the southern and northern regions. For instance, kurtosis (Fig.5 D) display wider distribution (negative kurtosis values) in the extreme North and Southwest regions, suggesting minor shifts in sorting- possibly related to autogenic forces.

Figure 8A compiles the grain-size metrics, provenance, and wind-direction from each transect in a schematic representation of Botucatu paleoerg. Southern transect exhibits a downwind grain-size coarsening due to lateral change in provenance (Figure 8B). Northeastern transect presents a downwind fining consistent with aeolian abrasion experimental data (Jerolmack et al., 2011). Northwestern transect have steady provenance and grain-size along downwind which suggests a mixture of sands from similar source rocks. The grain-size, provenance and wind-direction distribution of each transect are hypothesized to be controlled by three processes (Figure 9B): provenance (South transect), mixture (Northwestern transect) and aeolian abrasion (Northeastern transect). For grain-size controlled by provenance, the catchment rivers should display different sources along downwind direction (Figure 8C). This changes in provenance do not necessarily means sands sourced outside the basin but can be related to lateral facies or units changes in underlying strata. For grain-size be controlled by aeolian abrasion, there must not be a change in provenance on catchment rivers as well as a limited mixture of sands. For aeolian abrasion model, figure 8C proposes that a single catchment sourced the sand on upwind to the desert avoiding mixture of sources along downwind direction. The grain-size controlled by mixture occurs when the provenance does not change along downwind direction, but the mixtures of the abraded sands that have been transported in aeolian system and the "immature" sands from catchment rivers caps/stabilize the downwind fining.

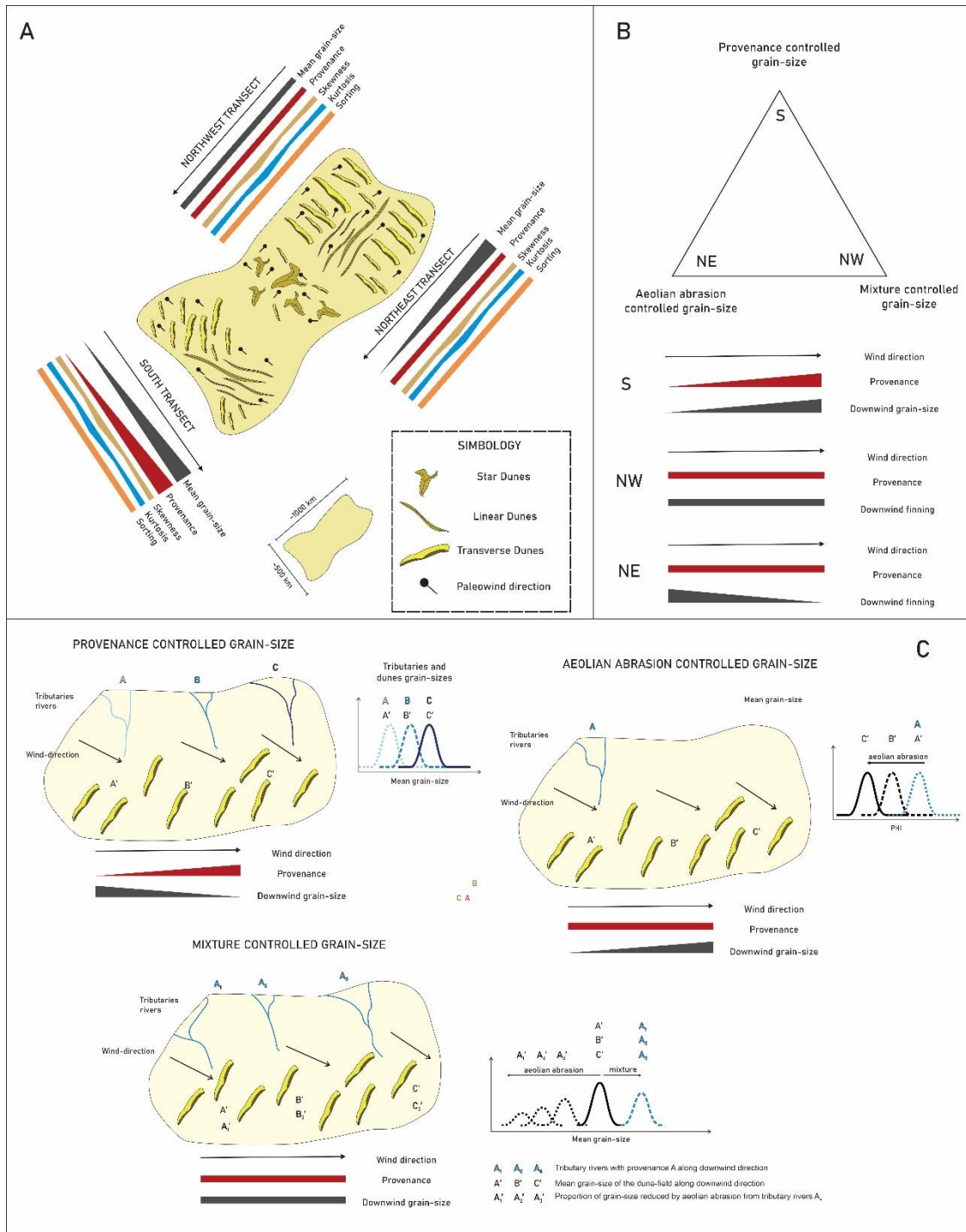


Figure 9 – Models for grain-size distribution along Botucatu paleoerg margins; A- grain-size metrics and provenance along the 3 transects (South, Northwest and Northeast) within Botucatu paleoerg; B- End-member process controlling the grain-size dispersion for each region and its characteristics; C- Provenance-, aeolian abrasion- and mixture control for grain-size in dune field schemes and relationship with catchment river detritus grain-size.

Considering the wind-direction, provenance and downwind trend tests, provenance changes are the most influential control spatial distribution of the grain-size in Botucatu Desert. When provenance changes on upwind, the dune-field mean grain-size mirrors

these changes in source rocks. Based on the recycled nature of the Botucatu sands (Bertolini et al., 2020) and the absence of extrabasinal sources – i.e. 1st cycle grains from basement rocks or sands transported from outside of the basin- it is considered that changes in the composition of the underlying Paraná Basin strata control the provenance of the Botucatu Desert. To the aeolian abrasion governs the dune-field grain-size, provenance must remain steady as well as a limited mixture of sources. Otherwise, provenance and mixture of sources shall overrule aeolian abrasion signal. In summary, the southeastern to southwestern coarsening and the grain-size interpolation map shows that provenance controls the granulometry distribution, while North transects display evidences of sand mixtures and aeolian abrasion. Autogenic forces do occur, but their influence appears to be localized and prone to be removed due to mixing of sands along input points desert margins.

5.1 Allogenic and autogenic controls in grain-size in Botucatu

Dune fields develop under allogenic (environmental factors) and autogenic (self-organization) conditions. In the aeolian realm, the autogenic process is exemplified by dune interactions, deformation during migration, scour of the substrate, or grain-size selection/abrasion (Bridge and Best, 1997; Cardenas et al., 2019; Coleman and Melville, 1996; Ewing et al., 2015; Gao et al., 2015a; Lancaster, 1986, 1981; Pedersen et al., 2015; Swanson et al., 2019, 2016; Werner, 1999; Zhang and Dong, 2015). Allogenic factors relate to the water-table rise/fall, wind and transport direction, source of sand, sand availability (Crabaugh and Kocurek, 1993; du Pont et al., 2014; Ewing et al., 2015; Gao et al., 2015b; Ping et al., 2014; Rubin and Hunter, 1987; Swanson et al., 2017). Allogenic factors are controlled, ultimately, by basin-scale tectonism, climate and base-level changes (Jerolmack and Paola, 2010; Rodríguez-López et al., 2014). Within the Botucatu paleoerg, the (1) bimodal wind-direction and (2) provenance sources are controlled by allogenic variables, whilst (3) downwind effects correspond to autogenic processes.

The wind model (figure 3) displays two end-member zones of different wind regimes controlled by global circulation patterns and the monsoonal climate (Moore et al., 1992; Scherer and Goldberg, 2007b). Grain size statistics (figure 3) show differences from north to south within the different wind regions. At first glance, these may represent an

wind-direction control on Botucatu paleoerg grain size distribution; however, apart from the southwestern samples, both the northern and southern regions have very similar mean grain-size and grain-size metrics (Figure 2). In contrast, provenance appears to have played an essential role in Botucatu paleoerg grain size dispersion, considering the overall E-W shift in provenance (Bertolini et al., 2021, 2020). Downwind fining in the northeastern region (Fig. 5 A) suggests that the autogenic process has at least some degree of control on grain-size. However, such effect is less dominant than the changes in provenance (allogenic), as revealed by downwind coarsening in the south, the lack of downwind fining in northwestern trend, and E-W grain-size trend in interpolation model (Fig. 6A).

Previous studies have determined that downwind fining is not always present in sediments transported by aeolian processes (Buckley, 1989; Livingstone et al., 1999; Sneh and Weissbrod, 1983; Warren, 1972). Although it should be noted that loess deposits appear to be spatially linked with sand seas (Crouvi et al., 2010, 2008). These deposits of coarse silt to very-fine sand, typically occur downwind of major sand seas (review in Crouvi et al. 2010). From an experimental aeolian transport perspective, studies (Durian et al., 2007, 2006; Roth et al., 2011) show that erosion drives the grains into a sphere independent of the original shape. However, erosion is a stationary process (Durian et al., 2007), meaning that after a grain reaches a determinate rounding degree, the process loses its effectiveness. Furthermore, (Kuenen, 1960) experiments on aeolian abrasion find a positive correlation of angularity, grain size, and surface roughness with aeolian abrasion rates. The experimental results demonstrate that the fining of sands is very dependent on the angularity of the grains- where rounded grains chip harder than very angular sands. Botucatu sands are comprised of multicycle sands- i.e. sands that have been deposited and reworked several times- thus, the sand grains are rounded prior to entering the sand sea. For instance, in the SW Botucatu region a mean of 9% of angular grains was recorded by Bertolini et al (2020), as such, only 9% of the grains are susceptible to intense spallation. Most Botucatu paleoerg sands are sub-rounded to sub-angular, agreeing with other deserts (Goudie and Watson, 1981). In such case, the effects of downwind fining are constrained by the available recycled sands from the underlying Paraná Basin sandstones. In summary, the strongly reworked sands available to the Botucatu aeolian system limits regional scale grain size fining.

The sorting, skewness and kurtosis interpolation models (Fig.6 B, C, D) finds regional clusters (from 50 to 100 km), which may show that downwind fining may still operate at smaller scales. Previous studies ((Jerolmack et al., 2011; Langford et al., 2016;

Livingstone et al., 1999)) show variations of around 5 to 30 km which is compatible with the clusters found. However, the regional nature of our dataset limits a more local evaluation. The local sources of sand across Botucatu (Bertolini et al., 2021, 2020), marked by heavy mineral peaks, suggest that local eroded sand was mixed with “abraded” sands that are already in the aeolian system.

In the Botucatu paleoerg, the allogenic controls on the provenance tend to be the most influential factor in grain size distribution (Figures 6 and 7). The provenance sources are controlled by the underlying distribution of Paraná Basin strata. The wind direction and wind strength are not influential of Botucatu granulometry dispersion. Consequently, the available grain size provided by underlying strata is the primary control on the grain size distribution in the Botucatu desert. Such conclusion is in contrast to Jerolmack & Brzinski III threshold sand sea hypothesis, which states that “*predominant grain size in a sand sea represents particles that are not too far above the threshold for entrainment under the dominant wind*” (Jerolmack et al., 2011; Jerolmack and Brzinski, 2010). The Southern Botucatu registers a downwind coarsening trend which shows that the same dominant wind can potentially carry different sand sizes- ruled by the change of provenance. Thus, there is not a single threshold for sand entrainment, but several considering that each provenance zone has its own energy potential rather than a single one for the erg. The available sand for the southern Botucatu region is derived from erosion of underlying strata which change laterally, which is a control that is difficult to incorporate into the threshold sand sea hypothesis. The conundrum is that ultimately the threshold hypothesis implies that the grain-size in a sand sea is governed by wind-strength, in some cases as in the Botucatu desert, however, the wind should be able to carry coarser sands, but the available sand is finer. For a sand sea to be ruled by the threshold hypothesis, the available sand should always be coarser than the threshold grain size for entrainment in the predominant wind. If the entrainment energy of the available sands is lower than the energy of the predominant wind, the provenance changes rule the predominant particle size in a sand sea.

The threshold hypothesis can operate in small-scale deserts such as the White Sands (~400 km²) or singled-sourced deserts, but for large-scale deserts such as the Botucatu (~1,000,000 km²) the number and magnitude of sources and their mixtures across the dominant wind need to be considered. Furthermore, to predict the mixture of sources in sand seas can be difficult due to different geological/geomorphic factors that may be unique to each desert (Farrant et al., 2019; Garzanti et al., 2021, 2020; Pastore et al., 2021; Rittner et al., 2016). An alternative interpretation for the the sand sea threshold hypothesis, is to consider that n sources of sand within a desert are ruled by

the hypothesis individually, while the predominant grain-size in a sand sea should be a product of the mixture of these n sources after the effects of sorting and fining downwind.

For autogenic processes, grain abrasion by particle-particle or particle-bed shock is experimentally proved to govern sands size and shape in aeolian transport, but only the northeastern region displays a downwind fining trend. The 0.4 μm per kilometre downwind fining is one magnitude order below those registered in the gypsum-sands of White Sands Dunefield (Langford et al., 2016). Three main reasons are hypothesized for the lower abrasion rates: (1) hardness difference from quartz to gypsum sands; (2) low angularity of the multicycle sands of the Botucatu; (3) scale differences from the 5 to 10 km transects from Jerolmack et al. (2011) and Langford et al. (2016) compared to this study 400 km transect. Due to the open nature of the desert, where sand can be supplied around desert margins, sand mixing will limit strong downwind fining patterns. However, the spatial distributions of sorting, skewness and kurtosis suggest that autogenic processes do occur but at a more local scale.

6. Conclusion

Based on forty-one granulometry samples from cross-stratified sandstones of the Botucatu paleoerg in Brazil, Uruguay and Namibia, we detailed the spatial distribution of grain size in an ancient large-scale dune field. Furthermore, we assess the grain size distribution with a paleowind direction model, based on previously published paleodirection data obtained in sandstones palaeodunes. From these data we conclude that:

- Minor to non-existent changes in granulometry are related to zones with different predominant winds;
- Basin-scale grain-size changes were controlled primarily by provenance sources rather than by wind-direction, downwind fining or sorting due abrasion during transport;
- Available recycled sand controls the grain-size distribution;
- Re-cycled and rounded sands and mixture of sources limits the downwind fining;
- Downwind selection effects probably limited to local scale, within 50-100 km;

Uncited references

(Langford et al., 2016)

(Jerolmack et al., 2011)

(Lancaster, 1986)

(Lancaster, 1989)

(Livingstone et al., 1999)

References

- Ahlbrandt, T.S., 1979. Textural parameters of eolian deposits. A Study Glob. Sand Seas Geol. Surv. Prof. Pap. 1052 1052, 429.
- Bagnold, R.A.F.R., 2016. The physics of blown sand and desert dunes.
- Baksi, A.K., 2018. Paraná flood basalt volcanism primarily limited to ~ 1 Myr beginning at 135 Ma: New $^{40}\text{Ar}/^{39}\text{Ar}$ ages for rocks from Rio Grande do Sul, and critical evaluation of published radiometric data. *J. Volcanol. Geotherm. Res.* 355, 66–77. <https://doi.org/10.1016/j.jvolgeores.2017.02.016>
- Bertolini, G., Marques, J.C., Hartley, A.J., Basei, M.A.S., Frantz, J.C., Santos, P.R., 2021. Determining sediment provenance history in a Gondwanan erg: Botucatu formation, Northern Paraná Basin, Brazil. *Sediment. Geol.* 417, 105883. <https://doi.org/10.1016/j.sedgeo.2021.105883>
- Bertolini, G., Marques, J.C., Hartley, A.J., Da-Rosa, A.A.S., Scherer, C.M.S., Basei, M.A.S., Frantz, J.C., 2020. Controls on Early Cretaceous desert sediment provenance in south-west Gondwana, Botucatu Formation (Brazil and Uruguay). *Sedimentology* 67, 2672–2690. <https://doi.org/10.1111/sed.12715>
- Bigarella, J.J., Oliveira, M.A.M. de, 1966. Nota preliminar sobre as direções de transporte dos arenitos Furnas e Botucatu na parte setentrional da Bacia do Paraná. *Bol. Parana. Geogr.* 18, 20.
- Bigarella, J.J., Salamuni, R., 1961. Early mesozoic wind patterns as suggested by dune bedding in the botucatú sandstone of Brazil and Uruguay. *Bull. Geol. Soc. Am.* 72, 1089–1105. [https://doi.org/10.1130/0016-7606\(1961\)72\[1089:EMWPAS\]2.0.CO;2](https://doi.org/10.1130/0016-7606(1961)72[1089:EMWPAS]2.0.CO;2)
- Bigarella, J.J., Van Eeden, O.R., 1970. Mesozoic palaeowind patterns and the problem of continental drift. *Bol. Parana. Geociências* 28, 115–144.
- Blott, S.J., Pye, K., 2001. Gradistat: A grain size distribution and statistics package for the analysis of unconsolidated sediments. *Earth Surf. Process. Landforms* 26,

1237–1248. <https://doi.org/10.1002/esp.261>

- Bridge, J., Best, J., 1997. Preservation of planar laminae due to migration of low-relief bed waves over aggrading upper-stage plane beds: Comparison of experimental data with theory. *Sedimentology*. <https://doi.org/10.1111/j.1365-3091.1997.tb01523.x>
- Bristow, C., Livingstone, I., 2019. Dune Sediments, in: *Aeolian Geomorphology: A New Introduction*. John Wiley & Sons Chichester, pp. 209–236.
- Buckley, R., 1989. Grain-size characteristics of linear dunes in central Australia. *J. Arid Environ.* 16, 23–28. [https://doi.org/10.1016/s0140-1963\(18\)31043-7](https://doi.org/10.1016/s0140-1963(18)31043-7)
- Bullard, J.E., McTainsh, G.H., Pudmenzky, C., 2004a. Aeolian abrasion and modes of fine particle production from natural red dune sands: An experimental study. *Sedimentology* 51, 1103–1125. <https://doi.org/10.1111/j.1365-3091.2004.00662.x>
- Bullard, J.E., McTainsh, G.H., Pudmenzky, C., 2004b. Aeolian abrasion and modes of fine particle production from natural red dune sands: An experimental study. *Sedimentology* 51, 1103–1125. <https://doi.org/10.1111/j.1365-3091.2004.00662.x>
- Bullard, J.E., Thomas, D.S.G., Livingstone, I., Wiggs, G.S.F., 1997. Dunefield Activity and Interactions with Climatic Variability in the Southwest Kalahari Desert. *Earth Surf. Process. Landforms* 22, 165–174. [https://doi.org/10.1002/\(SICI\)1096-9837\(199702\)22:2<165::AID-ESP687>3.0.CO;2-9](https://doi.org/10.1002/(SICI)1096-9837(199702)22:2<165::AID-ESP687>3.0.CO;2-9)
- Canile, F.M., Babinski, M., Rocha-Campos, A.C., 2016. Evolution of the Carboniferous-Early Cretaceous units of Paraná Basin from provenance studies based on U-Pb, Hf and O isotopes from detrital zircons. *Gondwana Res.* 40, 142–169. <https://doi.org/10.1016/j.gr.2016.08.008>
- Cardenas, B.T., Kocurek, G., Mohrig, D., Swanson, T., Hughes, C.M., Brothers, S.C., 2019. Preservation of Autogenic Processes and Allogenic Forcings in Set-Scale Aeolian Architecture II: The Scour-and-Fill Dominated Jurassic Page Sandstone, Arizona, U.S.A. *J. Sediment. Res.* 89, 741–760. <https://doi.org/10.2110/jsr.2019.41>
- Coleman, S., Melville, B., 1996. Initiation of Bed Forms on a Flat Sand Bed. *J. Hydraul. Eng.* 122, 301–310.
- Crabaugh, M., Kocurek, G., 1993. Entrada Sandstone: An example of a wet aeolian system. *Geol. Soc. Spec. Publ.* 72, 103–126. <https://doi.org/10.1144/GSL.SP.1993.072.01.11>

- Crouvi, O., Amit, R., Enzel, Y., Gillespie, A.R., 2010. Active sand seas and the formation of desert loess. *Quat. Sci. Rev.* 29, 2087–2098.
<https://doi.org/10.1016/j.quascirev.2010.04.026>
- Crouvi, O., Amit, R., Enzel, Y., Porat, N., Sandler, A., 2008. Sand dunes as a major proximal dust source for late Pleistocene loess in the Negev Desert, Israel. *Quat. Res.* 70, 275–282. <https://doi.org/10.1016/j.yqres.2008.04.011>
- de Assis Janasi, V., de Freitas, V.A., Heaman, L.H., 2011. The onset of flood basalt volcanism, Northern Paraná Basin, Brazil: A precise U-Pb baddeleyite/zircon age for a Chapecó-type dacite. *Earth Planet. Sci. Lett.* 302, 147–153.
<https://doi.org/10.1016/j.epsl.2010.12.005>
- du Pont, S.C., Narteau, C., Gao, X., 2014. Two modes for dune orientation. *Geology* 42, 743–746. <https://doi.org/10.1130/G35657.1>
- Durian, D.J., Bideaud, H., Düringer, P., Schröder, A., Thalmann, F., Marques, C.M., 2006. What is in a pebble shape? *Phys. Rev. Lett.* 97, 1–4.
<https://doi.org/10.1103/PhysRevLett.97.028001>
- Durian, D.J., Bideaud, H., Düringer, P., Schröder, A.P., Marques, C.M., 2007. Shape and erosion of pebbles. *Phys. Rev. E - Stat. Nonlinear, Soft Matter Phys.* 75, 1–9.
<https://doi.org/10.1103/PhysRevE.75.021301>
- Ernesto, M., Raposo, M.I.B., Marques, L.S., Renne, P.R., Diogo, L.A., Min, A. De, 1999. Paleomagnetism, geochemistry and $^{40}\text{Ar}/^{39}\text{Ar}$ dating of the North-eastern Parana Magmatic Province: Tectonic implications. *J. Geodyn.* 28, 321–340.
[https://doi.org/10.1016/S0264-3707\(99\)00013-7](https://doi.org/10.1016/S0264-3707(99)00013-7)
- Ewing, R.C., McDonald, G.D., Hayes, A.G., 2015. Multi-spatial analysis of aeolian dune-field patterns. *Geomorphology* 240, 44–53.
<https://doi.org/10.1016/J.GEOMORPH.2014.11.023>
- Farrant, A.R., Mounteney, I., Burton, A., Thomas, R.J., Roberts, N.M.W., Knox, R.W.O., Bide, T., 2019. Gone with the wind: Dune provenance and sediment recycling in the northern rub' al-khali, united arab emirates. *J. Geol. Soc. London.* 176, 269–283. <https://doi.org/10.1144/jgs2017-044>
- Folk, R.L., 1971. Longitudinal Dunes of the Northwestern Edge of the. *Sedimentology* 16, 5–54.
- Folk, R.L. and, Ward, W.C., 1957. Brazos River bar [Texas]; a study in the significance of grain size parameters. *J. Sediment. Petrol.* 27, 3–26.

- Fournier, J., Gallon, R.K., Paris, R., 2014. G2Sd: a new R package for the statistical analysis of unconsolidated sediments. *Géomorphologie Reli. Process. Environ.* 20, 73–78. <https://doi.org/10.4000/geomorphologie.10513>
- Francischini, H., Dentzien-Dias, P.C., Fernandes, M.A., Schultz, C.L., 2015. Dinosaur ichnofauna of the Upper Jurassic/Lower Cretaceous of the Paraná Basin (Brazil and Uruguay). *J. South Am. Earth Sci.* 63, 180–190. <https://doi.org/10.1016/j.jsames.2015.07.016>
- Gao, X., Narteau, C., Rozier, O., 2015a. Development and steady states of transverse dunes: A numerical analysis of dune pattern coarsening and giant dunes. *J. Geophys. Res. F Earth Surf.* <https://doi.org/10.1002/2015JF003549>
- Gao, X., Narteau, C., Rozier, O., Du Pont, S.C., 2015b. Phase diagrams of dune shape and orientation depending on sand availability. *Sci. Rep.* <https://doi.org/10.1038/srep14677>
- Garzanti, E., Andò, S., Vezzoli, G., Lustrino, M., Boni, M., Vermeesch, P., 2012. Petrology of the Namib Sand Sea: Long-distance transport and compositional variability in the wind-displaced Orange Delta. *Earth-Science Rev.* <https://doi.org/10.1016/j.earscirev.2012.02.008>
- Garzanti, E., Liang, W., Andò, S., Clift, P.D., Resentini, A., Vermeesch, P., Vezzoli, G., 2020. Provenance of Thal Desert sand: Focused erosion in the western Himalayan syntaxis and foreland-basin deposition driven by latest Quaternary climate change. *Earth-Science Rev.* <https://doi.org/10.1016/j.earscirev.2020.103220>
- Garzanti, E., Pastore, G., Stone, A., Vainer, S., Vermeesch, P., Resentini, A., 2021. Provenance of Kalahari Sand: Paleoweathering and recycling in a linked fluvial-aeolian system. *Earth-Science Rev.* 103867. <https://doi.org/10.1016/j.earscirev.2021.103867>
- Goudie, A. S., Allchin, B., Hegde, K. T. M., 1973. The Former Extensions of the Great Indian Sand Desert. *Author. R. Geogr. Soc.* 139, 243–257.
- Goudie, A.S., Watson, A., 1981. The shape of desert sand dune grains. *J. Arid Environ.* 4, 185–190. [https://doi.org/10.1016/s0140-1963\(18\)31559-3](https://doi.org/10.1016/s0140-1963(18)31559-3)
- Jerolmack, D.J., Brzinski, T.A., 2010. Equivalence of abrupt grain-size transitions in alluvial rivers and eolian sand seas: A hypothesis. *Geology* 38, 719–722. <https://doi.org/10.1130/G30922.1>

- Jerolmack, D.J., Paola, C., 2010. Shredding of environmental signals by sediment transport. *Geophys. Res. Lett.* 37, 1–5. <https://doi.org/10.1029/2010GL044638>
- Jerolmack, D.J., Reitz, M.D., Martin, R.L., 2011. Sorting out abrasion in a gypsum dune field. *J. Geophys. Res. Earth Surf.* 116, 1–15. <https://doi.org/10.1029/2010JF001821>
- Kocsis, A.T., Raja, N.B., 2020. Introduction to the ‘chronosphere’R package.
- Kocurek, G., Ewing, R.C., 2005. Aeolian dune field self-organization - Implications for the formation of simple versus complex dune-field patterns. *Geomorphology* 72, 94–105. <https://doi.org/10.1016/j.geomorph.2005.05.005>
- Kuenen, P.H., 1960. Experimental Abrasion 4: Eolian Action. *J. Geol.* 68, 427–449. <https://doi.org/10.1086/626675>
- Lancaster, N., 1989. *The Namib Sand Sea: dune forms, processes and sediments.* Balkema.
- Lancaster, N., 1986. Grain-size characteristics of linear dunes in the southwestern Kalahari. *J. Sediment. Petrol.* 56, 395–400. <https://doi.org/10.1306/212F8927-2B24-11D7-8648000102C1865D>
- Lancaster, N., 1985. Winds and sand movements in the Namib Sand Sea. *Earth Surf. Process. Landforms* 10, 607–619. <https://doi.org/10.1002/esp.3290100608>
- Lancaster, N., 1982. Dunes on the skeleton coast, Namibia (South West Africa): Geomorphology and grain size relationships. *Earth Surf. Process. Landforms* 7, 575–587. <https://doi.org/10.1002/esp.3290070606>
- Lancaster, N., 1981. Grain size characteristics of Namib Desert linear dunes. *Sedimentology* 28, 115–122. <https://doi.org/10.1111/j.1365-3091.1981.tb01668.x>
- Langford, R.P., Gill, T.E., Jones, S.B., 2016. Transport and mixing of eolian sand from local sources resulting in variations in grain size in a gypsum dune field, White Sands, New Mexico, USA. *Sediment. Geol.* 333, 184–197. <https://doi.org/10.1016/j.sedgeo.2015.12.010>
- Liang, A., Dong, Z., Qu, J., Su, Z., Wu, B., Zhang, Z., Qian, G., Gao, J., Pang, Y., Yang, Z., 2020. Using spatial variations of grain size to reveal sediment transport in the Kumtagh Sand Sea, Northwest China. *Aeolian Res.* 46, 100599. <https://doi.org/10.1016/j.aeolia.2020.100599>
- Livingstone, I., 1987. Grain-size variation on a “complex” linear dune in the Namib

- Desert. Geol. Soc. Spec. Publ. 35, 281–291.
<https://doi.org/10.1144/GSL.SP.1987.035.01.19>
- Livingstone, I.A.N., Bullard, J.E., Wiggs, G.F.S., Thomas, D.S.G., 1999. Grain-size variation on dunes in the southwest kalahari, Southern Africa. *J. Sediment. Res.* 69, 546–552. <https://doi.org/10.2110/jsr.69.546>
- Moore, G.T., Hayashida, D.N., Ross, C.A., Jacobson, S.R., 1992. Paleoclimate of the Kimmeridgian/Tithonian (Late Jurassic) world: I. Results using a general circulation model. *Palaeogeogr. Palaeoclimatol. Palaeoecol.* 93, 113–150.
[https://doi.org/10.1016/0031-0182\(92\)90186-9](https://doi.org/10.1016/0031-0182(92)90186-9)
- Mountney, Howell, 2000. Aeolian architecture, bedform climbing and preservation space in the Cretaceous Etjo Formation, NW Namibia. *Sedimentology* 47, 825–849. <https://doi.org/10.1046/j.1365-3091.2000.00318.x>
- Pastore, G., Baird, T., Vermeesch, P., Resentini, A., Garzanti, E., 2021. Provenance and recycling of Sahara Desert sand. *Earth-Science Rev.* 216, 103606.
<https://doi.org/10.1016/j.earscirev.2021.103606>
- Pebesma, E., Bivand, R.S., 2005. S classes and methods for spatial data: the sp package. *R news* 5, 9–13.
- Pebesma, E.J., 2018. Simple features for R: standardized support for spatial vector data. *R J.* 10, 439.
- Pedersen, A., Kocurek, G., Mohrig, D., Smith, V., 2015. Dune deformation in a multi-directional wind regime: White Sands Dune Field, New Mexico. *Earth Surf. Process. Landforms* 40, 925–941. <https://doi.org/10.1002/esp.3700>
- Ping, L., Narteau, C., Dong, Z., Zhang, Z., Courrech Du Pont, S., 2014. Emergence of oblique dunes in a landscape-scale experiment. *Nat. Geosci.* 7, 99–103.
<https://doi.org/10.1038/ngeo2047>
- Pinto, V.M., Hartmann, L.A., Santos, J.O.S., McNaughton, N.J., Wildner, W., 2011. Zircon U-Pb geochronology from the Paraná bimodal volcanic province support a brief eruptive cycle at ~135Ma. *Chem. Geol.* 281, 93–102.
<https://doi.org/10.1016/j.chemgeo.2010.11.031>
- R Core Team, 2021. *R: A Language and Environment for Statistical Computing.*
- Rittner, M., Vermeesch, P., Carter, A., Bird, A., Stevens, T., Garzanti, E., Andò, S., Vezzoli, G., Dutt, R., Xu, Z., Lu, H., 2016. The provenance of Taklamakan desert

sand. *Earth Planet. Sci. Lett.* 437, 127–137.
<https://doi.org/10.1016/j.epsl.2015.12.036>

Rodríguez-López, J.P., Clemmensen, L.B., Lancaster, N., Mountney, N.P., Veiga, G.D., 2014. Archean to Recent aeolian sand systems and their sedimentary record: Current understanding and future prospects. *Sedimentology* 61, 1487–1534. <https://doi.org/10.1111/sed.12123>

Roth, A.E., Marques, C.M., Durian, D.J., 2011. Abrasion of flat rotating shapes. *Phys. Rev. E - Stat. Nonlinear, Soft Matter Phys.* 83.
<https://doi.org/10.1103/PhysRevE.83.031303>

Rubin, D.M., Hunter, R.E., 1987. Bedform alignment in directionally varying flows. *Science (80-.)*. 237, 276–278. <https://doi.org/10.1126/science.237.4812.276>

Scherer, C.M.S., 2002. Preservation of aeolian genetic units by lava flows in the Lower Cretaceous of the Paraná Basin, Southern Brazil. *Sedimentology* 49, 97–116.
<https://doi.org/10.1046/j.1365-3091.2002.00434.x>

Scherer, C.M.S., 2000. Eolian dunes of the Botucatu Formation (Cretaceous) in southernmost Brazil: Morphology and origin. *Sediment. Geol.* 137, 63–84.
[https://doi.org/10.1016/S0037-0738\(00\)00135-4](https://doi.org/10.1016/S0037-0738(00)00135-4)

Scherer, C.M.S., Goldberg, K., 2007a. Palaeowind patterns during the latest Jurassic–earliest Cretaceous in Gondwana: Evidence from aeolian cross-strata of the Botucatu Formation, Brazil. *Palaeogeogr. Palaeoclimatol. Palaeoecol.* 250, 89–100. <https://doi.org/10.1016/j.palaeo.2007.02.018>

Scherer, C.M.S., Goldberg, K., 2007b. Palaeowind patterns during the latest Jurassic–earliest Cretaceous in Gondwana: Evidence from aeolian cross-strata of the Botucatu Formation, Brazil. *Palaeogeogr. Palaeoclimatol. Palaeoecol.* 250, 89–100. <https://doi.org/10.1016/j.palaeo.2007.02.018>

Scherer, C.M.S., Lavina, E.L.C., 2006. Stratigraphic evolution of a fluvial-eolian succession: The example of the Upper Jurassic–Lower Cretaceous Guar and Botucatu formations, Paran Basin, Southernmost Brazil. *Gondwana Res.* 9, 475–484. <https://doi.org/10.1016/j.gr.2005.12.002>

Silva, F.G., Scherer, C.M.S., 2000. Fcies, Associao de Fcies e Modelo Depositional dos Arenitos Elios da Formao Botucatu (Cretceo Inferior) na Regio Sul de Santa Catarina. *Pesqui. em Geocincias* 27, 15.
<https://doi.org/10.22456/1807-9806.20187>

- Sneh, A., Weissbrod, T., 1983. Size-frequency distribution of longitudinal dune rippled flank sands compared to that of slipface sands of various dune types. *Sedimentology* 30, 717–725. <https://doi.org/10.1111/j.1365-3091.1983.tb00705.x>
- Swanson, T., Mohrig, D., Kocurek, G., 2016. Aeolian dune sediment flux variability over an annual cycle of wind. *Sedimentology* 63, 1753–1764. <https://doi.org/10.1111/SED.12287>
- Swanson, T., Mohrig, D., Kocurek, G., Cardenas, B.T., Wolinsky, M.A., 2019. Preservation of autogenic processes and allogenic forcings in set-scale aeolian architecture I: Numerical experiments. *J. Sediment. Res.* 89, 728–740. <https://doi.org/10.2110/jsr.2019.42>
- Swanson, T., Mohrig, D., Kocurek, G., Liang, M., 2017. A Surface Model for Aeolian Dune Topography. *Math. Geosci.* 49, 635–655. <https://doi.org/10.1007/s11004-016-9654-x>
- Thiede, D.S., Vasconcelos, P.M., 2010. Paraná flood basalts: Rapid extrusion hypothesis confirmed by new $^{40}\text{Ar}/^{39}\text{Ar}$ results. *Geology* 38, 747–750. <https://doi.org/10.1130/G30919.1>
- Thomas, D.S.G., 1988. Analysis of linear dune sediment-form relationships in the Kalahari dune desert. *Earth Surf. Process. Landforms* 13, 545–553. <https://doi.org/10.1002/esp.3290130608>
- Tsoar, H., 1978. *The Dynamics of Longitudinal Dunes*.
- Vermeesch, P., 2013. Multi-sample comparison of detrital age distributions. *Chem. Geol.* 341, 140–146. <https://doi.org/10.1016/j.chemgeo.2013.01.010>
- Vermeesch, P., Garzanti, E., 2015. Making geological sense of “Big Data” in sedimentary provenance analysis. *Chem. Geol.* 409, 20–27. <https://doi.org/10.1016/j.chemgeo.2015.05.004>
- Wang, X., Dong, Z., Zhang, J., Qu, J., Zhao, A., 2003. Grain size characteristics of dune sands in the central Taklimakan Sand Sea. *Sediment. Geol.* 161, 1–14. [https://doi.org/10.1016/S0037-0738\(02\)00380-9](https://doi.org/10.1016/S0037-0738(02)00380-9)
- Warren, A., 1972. Observations on Dunes and Bi-Modal Sands in the Ténéré Desert. *Sedimentology* 19, 37–44. <https://doi.org/10.1111/j.1365-3091.1972.tb00234.x>
- Wasson, R.J., 1983. Dune sediment types, sand colour, sediment provenance and hydrology in the Strzelecki-Simpson dunefield, Australia. *Eolian sediments*

Process. 165–195.

Watson, A., 1986. Grain-size variations on a longitudinal dune and a barchan dune. *Sediment. Geol.* 46, 49–66. [https://doi.org/10.1016/0037-0738\(86\)90005-9](https://doi.org/10.1016/0037-0738(86)90005-9)

Werner, B.T., 1999. Complexity in natural landform patterns. *Science* (80-.). 284, 102–104. <https://doi.org/10.1126/science.284.5411.102>

Werner, B.T., 1995. Eolian dunes: computer simulations and attractor interpretation. *Geology* 23, 1107–1110. [https://doi.org/10.1130/0091-7613\(1995\)023<1107:EDCSAA>2.3.CO;2](https://doi.org/10.1130/0091-7613(1995)023<1107:EDCSAA>2.3.CO;2)

Wickham, H., Wickham, M.H., 2017. Package tidyverse. Easily Install Load 'Tidyverse.

Wilson, I.G., 1973. Ergs. *Sediment. Geol.* 10, 77–106. [https://doi.org/10.1016/0037-0738\(73\)90001-8](https://doi.org/10.1016/0037-0738(73)90001-8)

Zhang, Z., Dong, Z., 2015. Grain size characteristics in the Hexi Corridor Desert. *Aeolian Res.* 18, 55–67. <https://doi.org/10.1016/j.aeolia.2015.05.006>

Zhou, N., Li, Q., Zhang, C.-L., Chi-Hua, H., Wu, Y., Zhu, B., Cen, S., Huang, X., 2021. Grain size characteristics of aeolian sands and their implications for the aeolian dynamics of dunefields within a river valley on the southern Tibet Plateau: A case study from the Yarlung Zangbo river valley. *CATENA* 196, 104794. <https://doi.org/10.1016/j.catena.2020.104794>